

Seismic Performance Assessment of a Pin-bearing Restraint System for Curved Bridge

Huili Wang^{*1,2}, Kunkun Zhao¹, Sifeng Qin³

¹ National & Local Joint Engineering Laboratory of Bridge and Tunnel Technology, Dalian University of Technology, 116023 Dalian, China

² State Key Laboratory of Structural Analysis for Industrial Equipment, Dalian University of Technology, 116023 Dalian, China

³ College of Civil Engineering and Architecture, Dalian University, 116622 Dalian, China

* Corresponding author, e-mail: wanghuili@dlut.edu.cn

Received: 03 November 2021, Accepted: 21 June 2022, Published online: 13 July 2022

Abstract

The traditional restraint systems limit the deformation of curved bridge under temperature load, which results in radial and tangential secondary internal forces in the bridge. This paper proposes a pin-bearing restraint system (PBRS) for curved bridge, which can relax the rotational deformation of curved bridge under temperature load. Its configuration and working mechanism are illustrated. The finite element model of a curved bridge with PBRS is established using ANSYS software, and nonlinear time history analysis is conducted. The pounding force and pounding number between pin and slot under ground motion are analyzed. The pin stiffness, the gap and the ratio of upper structure mass to lower structure mass are selected for parametric study. The results show that the pounding force and pounding number present dramatic changes with pin stiffness. As the pin stiffness increases, the pounding force presents a logarithmic linear tendency, and the pounding number shows a reduce tendency. Gap has little influence on pounding force and pounding number. The radial pounding force and pounding number increase with the increase of mass ratio.

Keywords

curved bridge, bearing, restraint, FEM, time history analysis

1 Introduction

The curved bridge is widely used, especially in urban overpasses. However, diseases often occur around some curved bridges. The main cause is that the mechanical characteristics of curved bridge are different from those of straight bridge [1]. The bending-torsion coupling and uneven supporting force are the mechanical characteristics of curved bridge. Especially, the curved bridge could occur transversal movement under temperature load. Movements due to the temperature load must be allowed in the direction radiating from the support and the bearing must accommodate such movements [2]. However, the bridge would fail in earthquake without redundant constraints [3]. Since the San Fernando earthquake in California on February 9, 1971, the seismic performance of curved bridges has attracted much attention [4, 5]. Malhotra et al. [6] studied the mechanism of pounding between curved girder through shaking table test. Monzon et al. [7] carried out a large-scale model of a curved steel I-girder bridge with seismic isolation tested on multiple shaking tables to

determine the failure limit states. Kawashima et al. [8] reported that the collapse of curved Baihua bridge in the Wenchuan earthquake was mainly attributed to the insufficient support length of the transverse beam and lacking of longitudinal displacement restraints.

The support and restraint types are important for curved bridge. Samaan et al. [2] investigated the bearing arrangements and types in the design of continuous two-span girder prototype bridges. Galindo et al. [9] analyzed the effectiveness of seismic isolation, based on lead rubber bearings, with respect to the overall performance of curved highway viaducts. Guo et al. [10] proposed a restraint system with shear bolts for double-deck curved bridges. Ghosh et al. [11] evaluated the performance of four different types of protective devices to limit the displacement of the upper structure during earthquakes. Tanimura et al. [12] analyzed the three-dimensional dynamic behavior of a bridge and found that the velocity difference between the upper and the lower bridge bearings caused the fracture in bearing.

The traditional restraint systems limit the deformation of curved bridge under temperature load resulting in radial and tangential secondary internal forces. The temperature effect is the main factor causing the radial force of curved bridge [13]. There is difference in mechanical characteristics and deformation rules between curved bridge and straight bridge. However, the traditional restraint systems do not distinguish between curved bridge and straight bridge. The pin-bearing restraint system (PBRS) is presented in this paper, which not only accommodate the deformation caused by temperature but also prevent the falling of the beam during the earthquake. This paper aims to propose PBRS for curved bridge and analyze its seismic characteristics. The pounding force and pounding number are regarded as evaluation indexes of PBRS. The pin stiffness, the gap, and the ratio of upper structure mass to lower structure mass are selected for parametric study.

2 Construction of pin-bearing restraint system

The traditional restraint systems for curved bridge bearing arrangements are illustrated in Fig. 1. There are three types of supports in the middle pier, including full torsional support, middle hinge support and torsional-hinge support.

Due to the coupling deformation of bending and torsion, under the temperature load, not only tangential displacement but also radial displacement occur in the curved bridge, as shown in Fig. 2 [14]. However, the traditional horizontal restraint systems of curved bridge cannot relax the radial displacement.

The PBRS is proposed to limit the radial displacement, which can relax the tangential displacement and radial displacement, as shown in Fig. 3. Bidirectional movable support is set on each pier, which limits vertical displacement of the girder. Radial movable pin limits the tangential displacement and tangential movable pin limits the radial displacement. PBRS can restrain horizontal displacement of the girder depending on the gaps between the pin and slot. The horizontal load is borne by pin.

The structure of pin is shown in Fig. 4. A slot, which is welded with steel plates and shear studs, is embedded in the cap beam. A limit pin is installed under the beam. The pin is welded with arc-shaped steel plates and T-shaped stiffeners. The pin and beam are connected by embedded steel plates and shear studs. Gaps are set between the limit pin and slot to release the displacement constraints of beam, which are adjustable to meet the displacement requirements. The PBRS has been applied to practical projects, as shown in Fig. 5.

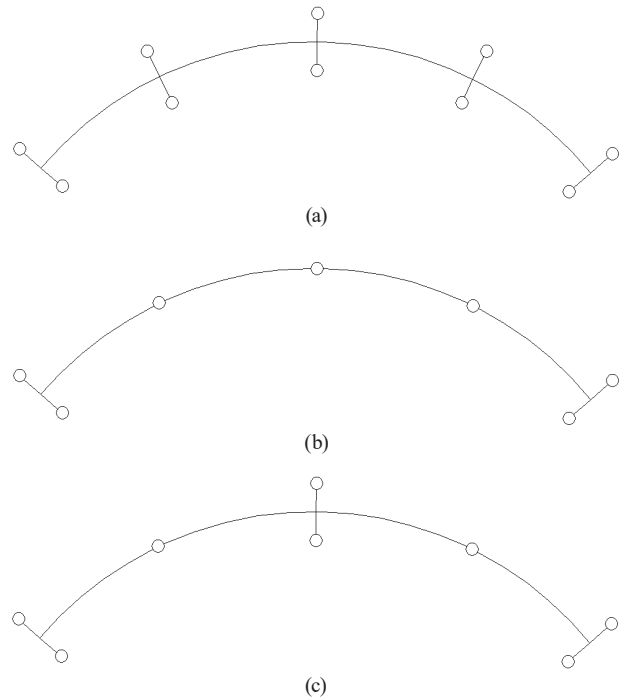


Fig. 1 Schematic plan of continuous curved bridge restraint system, (a) Full torsional support, (b) Middle hinge support, (c) Torsional-hinge support

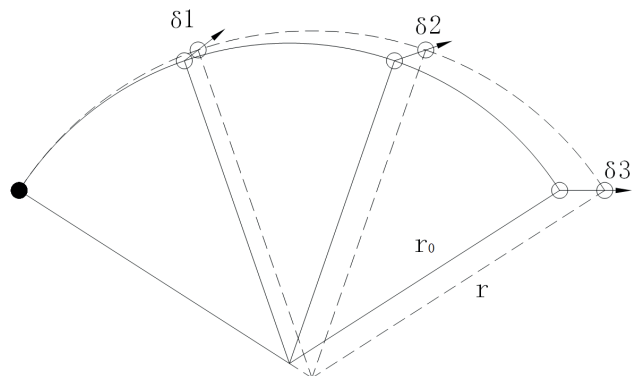


Fig. 2 Deformation plan diagram of curved beam under temperature load

PBRS can relax the rotational deformation of curved bridge under temperature load. However, the pin would collide with slot under earthquake load. The pounding force and pounding number would be surveyed in this paper.

3 Benchmark Bridge

A three-span curved bridge is considered in the present study. It is a continuous bridge with a span of 3×25 m, with a curvature radius of 60 m (Fig. 6). The box steel girder is 2 m high, 9 m wide with orthotropic steel bridge deck. The concrete pier is a 18 m high frame with solid rectangle section. A tangential movable pin is set on each of Pier A and Pier D. A radial movable radial pin is set on Pier B and a bidirectional movable pin is set on Pier C.

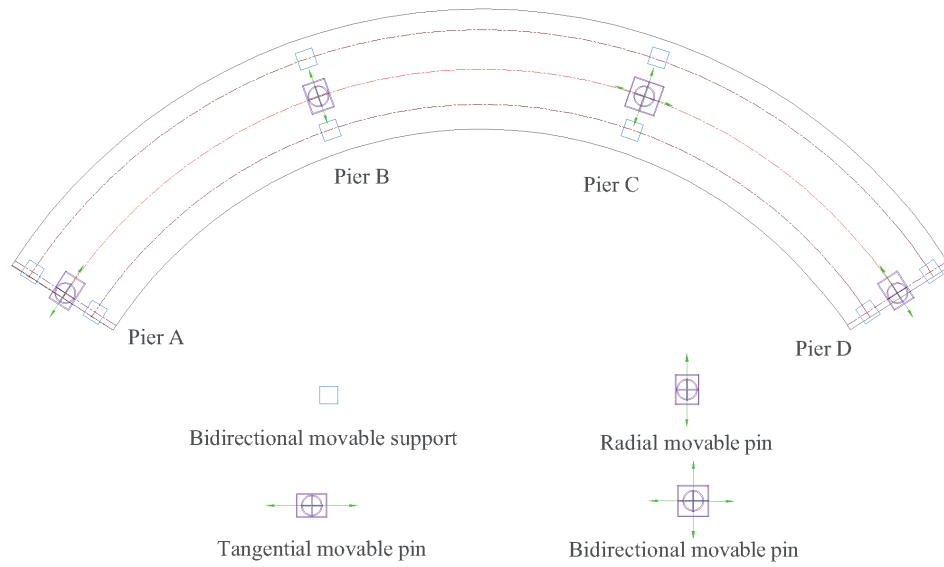


Fig. 3 Plane layout of a curved bridge with PBRS

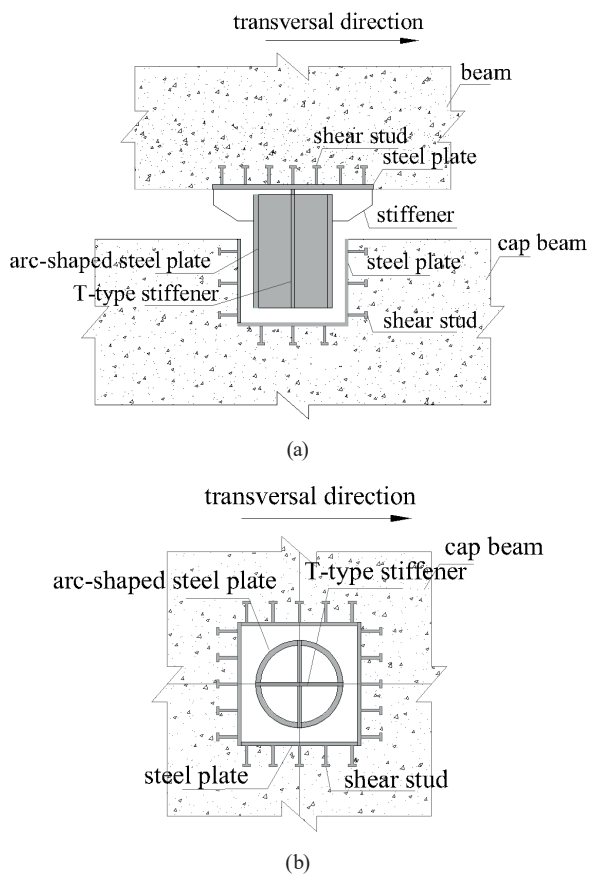


Fig. 4 Diagram of spacing slot and limit pin, (a) Elevation, (b) Plan



(a)



(b)

Fig. 5 PBRS in practice, (a) Limit pin, (b) Limit pin in slot

The sectional geometric properties are listed in Table 1. The yield strength of the girder steel (f_y) is 345 MPa. The strength of the pier concrete (f_c) is 29.2 MPa and the yield strength of reinforcement (f_y) is 345 MPa.

4 Number modeling

4.1 Pounding model

The pin and slot are simulated using Kelvin model, which is combined with a spring and a damper, as shown in Fig. 7 [15].

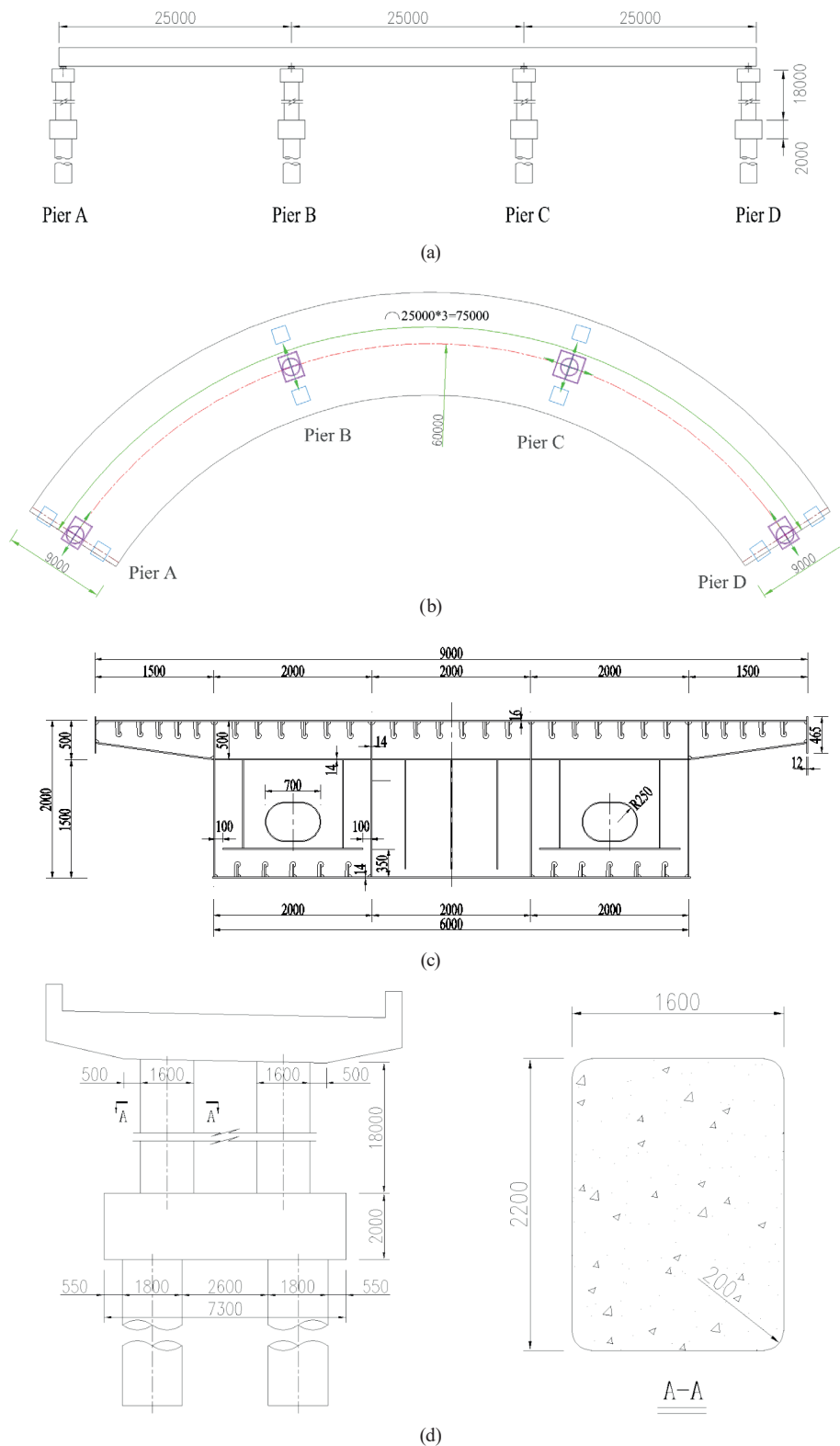


Fig. 6 Bridge layout schematic (mm), (a) Elevation, (b) Plan, (c) Girder cross section, (d) Pier

Table 1 Material and sectional geometric properties of the bridge

Section location	Section area/m ²	Moment of inertia about the transverse axis/m ⁴	Material	Elastic modulus E/GPa	Poisson's ratio μ	Density ρ / kg/m ³
Girder	0.193	0.196	steel	206	0.31	7850
Pier	3.486	1.381	concrete	32.5	0.20	2400

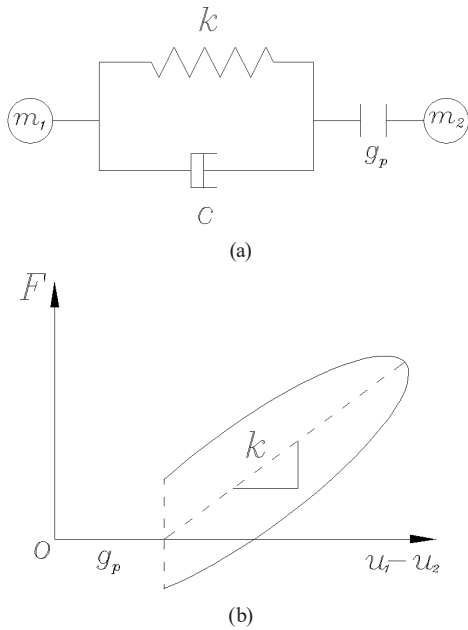


Fig. 7 Kelvin model (a) Schematic arrangement of constituent elements, (b) Force-displacement behavior

When the gap closes, the force transmits from one structure to another. The pin and slot would collide each other. The pin stiffness is simulated using the spring. The damper accounts for energy dissipation during collision. The force-displacement relationship is [16]

$$\begin{cases} F = k(u_1 - u_2 - g_p) + c(v_1 - v_2) & u_1 - u_2 - g_p \geq 0 \\ F = 0 & u_1 - u_2 - g_p < 0 \end{cases}, \quad (1)$$

where m_1 and m_2 represent masses of the limit pin and slot. u_1 and u_2 are the displacements of limit pin and slot. v_1 and v_2 are the velocities of limit pin and slot. g_p is the gap. k is the elastic stiffness constant of the limit pin.

Where damping coefficient

$$c = 2\zeta \sqrt{k \frac{m_1 m_2}{m_1 + m_2}} \quad (2)$$

$$\zeta = \frac{-\ln r}{\sqrt{(\ln r)^2 + \pi^2}} \quad (3)$$

r is the coefficient of restitution, which is obtained from the following equation.

$$r = \frac{v_2' - v_1'}{v_2 - v_1}, \quad (4)$$

where v_1 and v_2 are the corresponding velocities of the colliding masses (m_1 and m_2) before collision, v_1' and v_2' are the velocities after collision. In this paper, r is assumed as 0.65 [17].

The kinematic equation is

$$\begin{bmatrix} m_1 & 0 \\ 0 & m_2 \end{bmatrix} \begin{Bmatrix} \ddot{u}_1 \\ \ddot{u}_2 \end{Bmatrix} + \begin{bmatrix} c & -c \\ -c & c \end{bmatrix} \begin{Bmatrix} \dot{u}_1 \\ \dot{u}_2 \end{Bmatrix} + \begin{bmatrix} k & -k \\ -k & k \end{bmatrix} \begin{Bmatrix} u_1 \\ u_2 \end{Bmatrix} = \begin{Bmatrix} 0 \\ 0 \end{Bmatrix}. \quad (5)$$

4.2 FE model

The bridge structure has been modeled using the software ANSYS [18]. The upper structure and the piers have been modeled using 3D frame elements with mass concentrated at discrete points, as shown in Fig. 8(a). The girder and cap beam of the curved bridge are modeled using elastic beam-column elements because they are expected to remain elastic during seismic excitation. Elastomeric bearings have been modeled using elastic link elements. Since the piers are supported by rock, they have been modeled as fixed on the foundation. Two Kelvin models are used to simulate the pounding between limit pin and slot, as shown in Fig. 8(b).

4.3 Selection of the ground motions

According to the current guidelines for seismic design of highway bridges of China, the ground motion parameters of bridge engineering site are peak ground acceleration $PGA = 0.4 \text{ g}$ and the characteristic period $T_g = 0.4 \text{ s}$. Ground motions with high amplitude velocity pulse characteristic tend to produce response of the bridge structures [19]. The ground motions are selected from the motion data base in PEER [20] (Table 2). These records are scaled to a peak ground acceleration of 0.4 g, as shown in Fig. 9. It is important to note that the motion is applied along the vertical direction of the line between Pier A and Pier D.

5 Parametric study results and discussion

The pin and slot would collide under earthquake load, so the pounding force and pounding number are regarded as evaluation indexes for PBRS. A parametric study is conducted to examine the effect of pin stiffness (k) and the gap (g_p). The ratio of upper structure mass to lower structure mass affects the pounding force so the ratio (α) is also invested. They are divided into three groups, as listed in Table 3.

5.1 Influence of pin stiffness

In order to study the influence of pin stiffness, assume gap $g_p = 50 \text{ mm}$, mass ratio $\alpha = 1$. The pin stiffness varies from 1.13×10^1 to $1.13 \times 10^{13} \text{ kN/m}$. The pin stiffness (k) and peak value of pounding force (F) are plotted on the dual logarithmic coordinate diagram. The pounding number between pin and slot is plotted on the single logarithmic

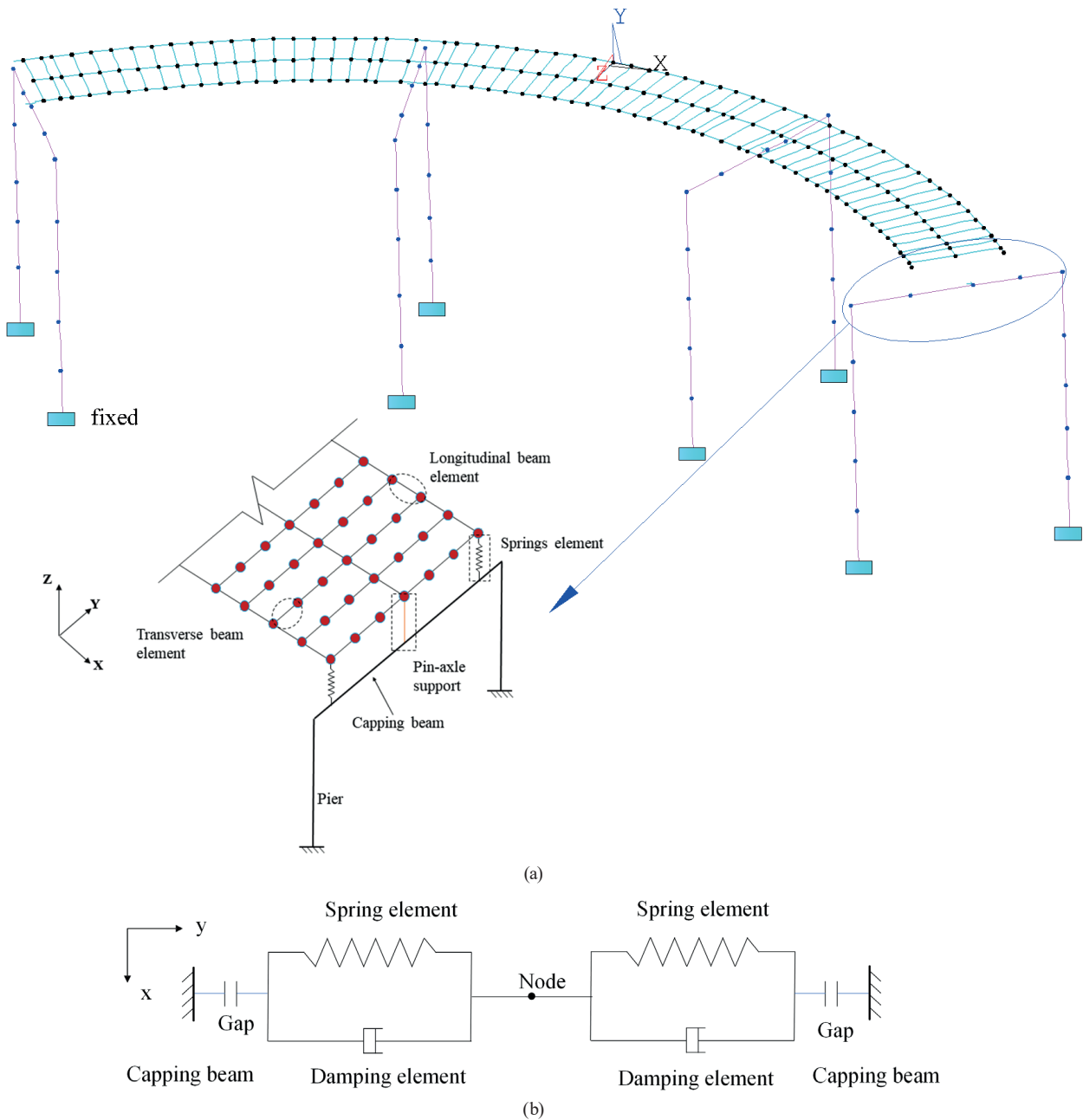


Fig. 8 3D FE model, (a) Sketch of skew bridge model, (b) PBR model

Table 2 Selected ground motion recorders

No.	Earthquake	Year	Station	PGA(g)	PGV(m/s)	T_g
1	Northridge	1994	Sylmar	0.416	0.417	0.642
2	Jame RD	1979	EI centro	0.507	0.361	0.456
3	Taft_h	1952		0.431	0.400	0.404

coordinate diagram, as shown in Fig. 10. It can be seen that the pounding force presents a logarithmic linear tendency as the pin stiffness increases. The peak value of pounding force presents dramatic changes with pin stiffness. This is because the internal force is positively associated with stiffness. The pounding number presents a reduce tendency

as the pin stiffness increases. Especially when the stiffness is larger than 10^7 KN/m, the pounding number dramatically decreases. As the stiffness becomes larger, the pounding force increases, so each pounding energy dissipation become larger. The earthquake energy is constant, therefore pounding number decreases.

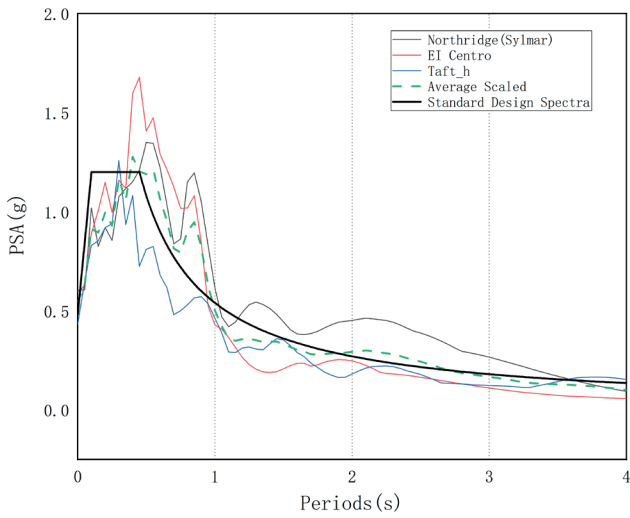


Fig. 9 Acceleration response spectrum of the selected ground motions

5.2 Influence of gap

In order to study the influence of gap, assume pin stiffness $\kappa = 1.13 \times 10^9$ KN/m, mass ratio $\alpha = 1$. The gap g_p varies from 10 to 50 mm. The peak value of pounding force and pounding number are plotted in Fig. 11. Gaps have little effect on pounding force because of stochastic behaviors of earthquakes. The radial pounding force

Table 3 Parametric study configurations

model	pin stiffness κ (kN/m)	gap g_p (mm)	mass ratio α	group
K1-G50-a1.0	1.13×10^1	50	1	
K3-G50-a1.0	1.13×10^3	50	1	
K5-G50-a1.0	1.13×10^5	50	1	
K7-G50-a1.0	1.13×10^7	50	1	M_k
K9-G50-a1.0	1.13×10^9	50	1	
K11-G50-a1.0	1.13×10^{11}	50	1	
K13-G50-a1.0	1.13×10^{13}	50	1	
K9-G10-a1.0	1.13×10^9	10	1	
K9-G20-a1.0	1.13×10^9	20	1	
K9-G30-a1.0	1.13×10^9	30	1	M_g
K9-G40-a1.0	1.13×10^9	40	1	
K9-G50-a1.0	1.13×10^9	50	1	
K9-G50-a0.5	1.13×10^9	50	0.5	
K9-G50-a1.0	1.13×10^9	50	1	
K9-G50-a1.5	1.13×10^9	50	1.5	M_a
K9-G50-a2.0	1.13×10^9	50	2	
K9-G50-a2.5	1.13×10^9	50	2.5	
K9-G50-a3.0	1.13×10^9	50	3	

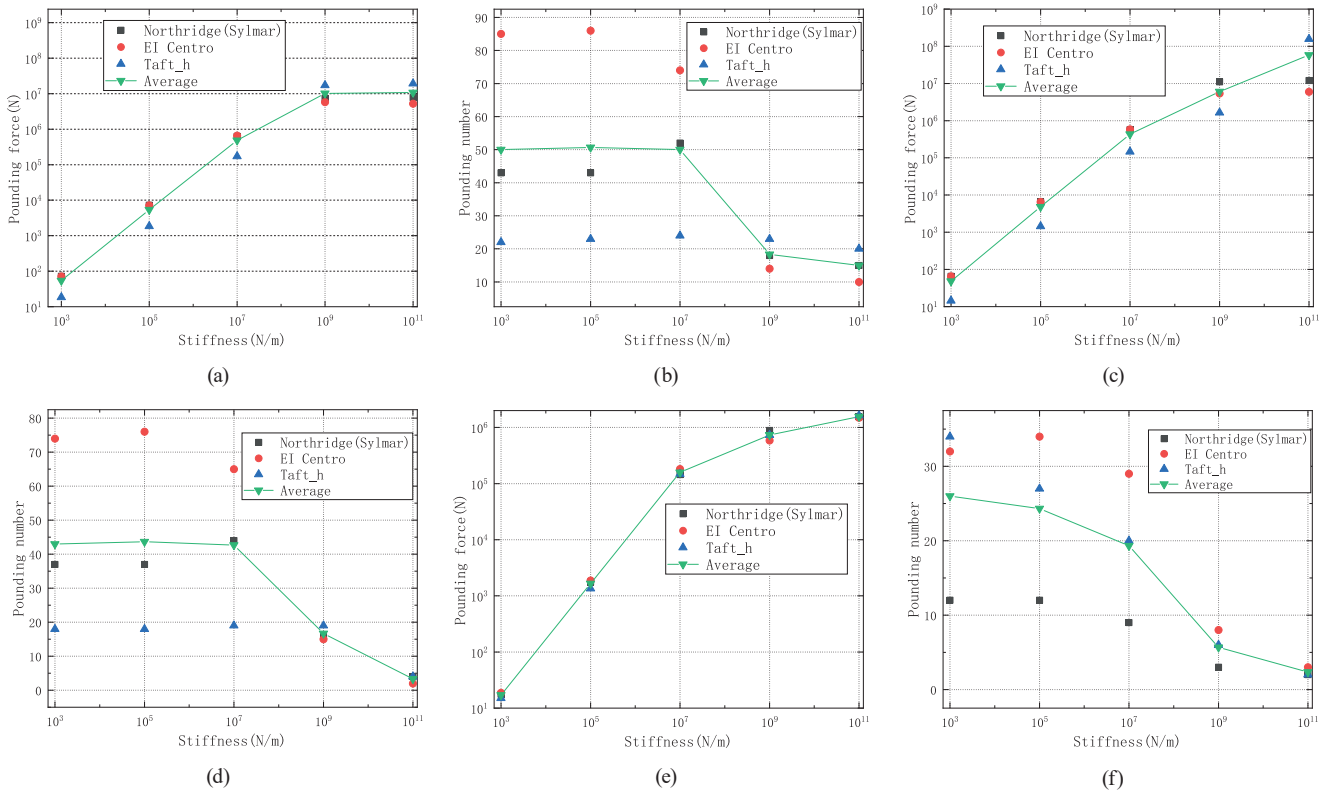


Fig. 10 Pounding force, pounding number vs. pin stiffness, (a) Radial pounding force of the pin on pier B, (b) Radial pounding number of the pin on pier B, (c) Radial pounding force of the pin on pier C, (d) Radial pounding number of the pin on pier C, (e) Tangential pounding force of the pin on pier C, (f) Tangential pounding number of the pin on pier C

overall decreases with the increase of gap. The tangential pounding force increases and then decreases with the increase of gap. The pounding number shows a decreasing tendency along with the increase of gap. The collision probability decreases with increase of gap. If the gap is larger than the displacement under earthquake, collision would not happen.

5.3 Influence of mass ratio

In order to study the influence of the mass ratio, assume pin stiffness $\kappa = 1.13 \times 10^9$ KN/m, gap $g_p = 50$ mm. The mass ratio α varies from 0.5 to 3.0. The peak value of pounding force and pounding number are plotted in Fig. 12. The radial pounding force and pounding number increase with increase of α . According to D'Alembert's principle, the increase of upper structure mass causes pounding force to increase. α has little effect on tangential pounding force and pounding number due to the stochastic behaviors of earthquakes.

6 Conclusions

In this paper, the pin-bearing restraint system (PBRs) for curved bridge is proposed. The configuration, working

mechanism and the force-deformation behavior of PBRs are introduced. The pounding force and pounding number between pin and slot under ground motion are analyzed. The effects of pin stiffness, the gap and the mass ratio are investigated. From the results, the following conclusions can be drawn:

1. The pounding force and pounding number present dramatic changes with pin stiffness. As the pin stiffness increases, the pounding force presents a logarithmic linear tendency, and the pounding number presents a reduce tendency.
2. Gap has little influence on pounding force. The pounding number decreases as the gap increases. Gap has little effect on pounding force and pounding number.
3. The radial pounding force and pounding number increase with the increase of mass ratio. Mass ratio has little effect on tangential pounding force and pounding number.

Conflict of interests

The authors declare that there is no conflict of interests regarding the publication of this paper.

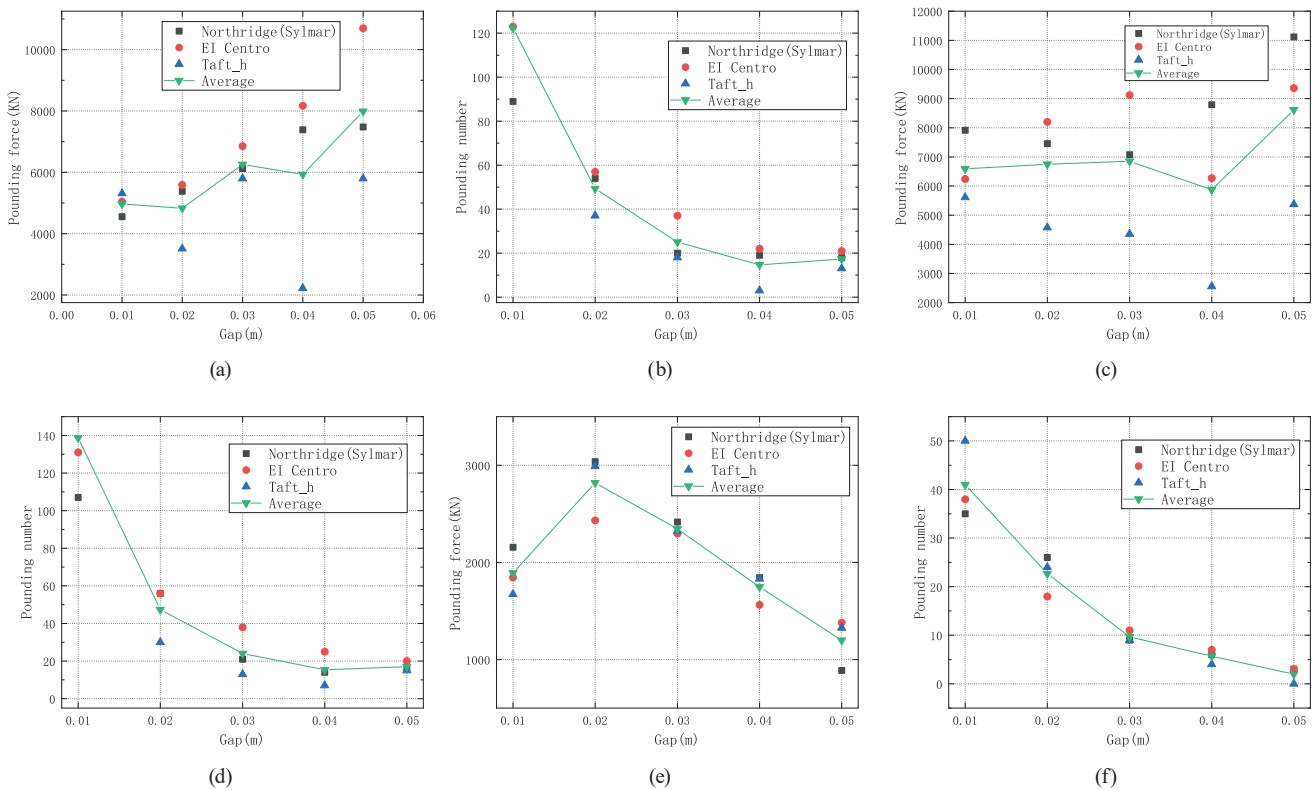


Fig. 11 Pounding force, pounding number vs. gap, (a) Radial pounding force of the pin on pier B, (b) Radial pounding number of the pin on pier B, (c) Radial pounding force of the pin on pier C, (d) Radial pounding number of the pin on pier C, (e) Tangential pounding force of the pin on pier C, (f) Tangential pounding number of the pin on pier C

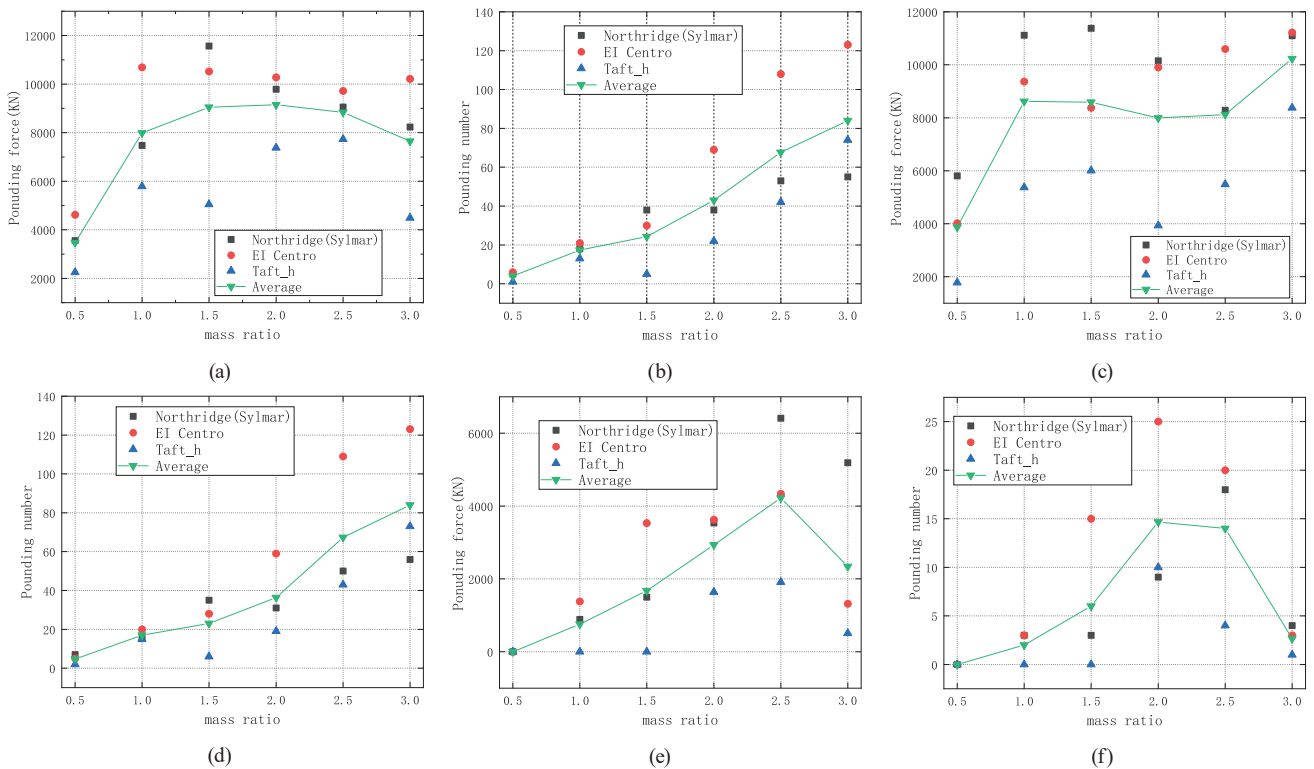


Fig. 12 Pounding force, pounding number vs. α , (a) Radial pounding force of the pin on pier B, (b) Radial pounding number of the pin on pier B, (c) Radial pounding force of the pin on pier C, (d) Radial pounding number of the pin on pier C, (e) Tangential pounding force of the pin on pier C, (f) Tangential pounding number of the pin on pier C

Data availability

All data, models, and code generated or used during the study appear in the submitted article.

Acknowledgments

This work is supported by the Doctoral Start-up Foundation of Liaoning Province (20170520138) and the Natural Science Foundation of Liaoning Province (2019-ZD-0006).

References

[1] Jiao, C., Liu, L., Long, P., Hou, S. "Creeping mechanism analysis of curved bridges", In: 10th Asia Pacific Transportation Development Conference, Beijing, China, 2014, pp. 639–646. <https://doi.org/10.1061/9780784413364.078>

[2] Samaan, M., Sennah, K., Kennedy, J. B. "Positioning of bearings for curved continuous spread-box girder bridges", Canadian Journal of Civil Engineering, 29(5), pp. 641–652, 2002. <https://doi.org/10.1139/102-049>

[3] Peng, T., Guo, Z. "A new design strategy for seismic safety in super earthquakes of continuous girder bridges", Measurement, 163, 108000, 2020. <https://doi.org/10.1016/j.measurement.2020.108000>

[4] Tseng, W. S., Penzien, J. "Seismic analysis of long multiple-span highway bridges", Earthquake Engineering and Structural Dynamics, 4(1), pp. 1–24, 1975. <https://doi.org/10.1002/eqe.4290040102>

[5] Williams, D., Godden, W. "Seismic response of long curved bridge structures: Experimental model studies", Earthquake Engineering and Structural Dynamics, 7(2), pp. 107–128, 1979. <https://doi.org/10.1002/eqe.4290070202>

[6] Malhotra, P. K., Huang, M. J., Shakal, A. F. "Seismic interaction at separation joints of an instrumented concrete bridge", Earthquake Engineering and Structural Dynamics, 24(8), pp. 1055–1067, 1995. <https://doi.org/10.1002/eqe.4290240802>

[7] Monzon, E. V., Buckle, I. G., Itani, A. M. "Seismic Performance and Response of Seismically Isolated Curved Steel I-Girder Bridge", Journal of Structural Engineering, 142(12), 04016121, 2016. [https://doi.org/10.1061/\(ASCE\)ST.1943-541X.0001594](https://doi.org/10.1061/(ASCE)ST.1943-541X.0001594)

[8] Kawashima, K., Takahashi, Y., Ge, H., Wu, Z., Zhang, J. "Reconnaissance Report on Damage of Bridges in 2008 Wenchuan, China, Earthquake", Journal of Earthquake Engineering, 13(7), pp. 965–996, 2009. <https://doi.org/10.1080/13632460902859169>

[9] Galindo, C. M., Belda, J. G., Hayashikawa, T. "Non-linear seismic dynamic response of curved steel bridges equipped with LRB supports", Steel Construction, 3(1), pp. 34–41, 2010. <https://doi.org/10.1002/stco.201010005>

[10] Guo, W., Lu, L., Whang, K. "Effect of Different Constraint Systems on the Seismic Response of Double-deck Curved Girder Bridges", Journal of Highway and Transportation Research and Development (English Ed.), 13(4), pp. 35–43, 2019. <https://doi.org/10.1061/JHTRCQ.0000702>

- [11] Ghosh, G., Singh, Y., Thakkar, S. K. "Seismic response of a continuous bridge with bearing protection devices", *Engineering Structures*, 33(4), pp. 1149–1156, 2011.
<https://doi.org/10.1016/j.engstruct.2010.12.033>
- [12] Tanimura, S., Sato, T., Umeda, T., Mimura, K., Yoshikawa, O. "A note on dynamic fracture of the bridge bearing due to the great Hanshin – Awaji earthquake", *International Journal of Impact Engineering* 27(2), pp. 153–160, 2002.
[https://doi.org/10.1016/S0734-743X\(01\)00037-9](https://doi.org/10.1016/S0734-743X(01)00037-9)
- [13] Tian, Y., Zhang, N., Xia, H. "Temperature effect on service performance of high-speed railway concrete bridges", *Advances in Structural Engineering*, 20(6), pp. 865–883, 2017.
<https://doi.org/10.1177/1369433216665306>
- [14] Kim, S.-H., Lee, Y.-S., Cho, K.-Y. "Analysis of Horizontal Reactions Due to Moving Vehicle Loads in Curved Bridges with Varied Support Conditions", *Advances in Structural Engineering*, 8(5), pp. 529–545, 2005.
<https://doi.org/10.1260/136943305774858025>
- [15] Blandon, C. A., Priestley, M. J. N. "Equivalent viscous damping equations for direct displacement based design", *Journal of Earthquake Engineering*, 9(2), pp. 257–278, 2005.
<https://doi.org/10.1142/S1363246905002390>
- [16] Ye, K., Li, L., Zhu, H. "A modified Kelvin impact model for pounding simulation of base-isolated building with adjacent structures", *Earthquake Engineering and Engineering Vibration*, 2009, 8(3), pp. 433–446, 2009.
<https://doi.org/10.1007/s11803-009-8045-4>
- [17] Anagnostopoulos, S. A. "Pounding of buildings in series during earthquakes", *Earthquake Engineering and Structural Dynamics*, 16(3), pp. 443–456, 1998.
<https://doi.org/10.1002/eqe.4290160311>
- [18] ANSYS "ANSYS 2021 R1" [online] Available at: <https://www.ansys.com/>
- [19] Chen, J., Han, Q., Liang, X., Du, X. "Effect of pounding on nonlinear seismic response of skewed highway bridges", *Soil Dynamics and Earthquake Engineering*, 103, pp. 151–165, 2017.
<https://doi.org/10.1016/j.soildyn.2017.09.008>
- [20] UC Berkeley "Data Sciences" [online] Available at: <https://peer.berkeley.edu/research/data-sciences>